by a CN group of the cyanide complexes, thereby giving rise to a CN-bridged ion pair (Figure 3). The slight enhancement of the $[Tb\subset 2.2.1]^{3+}$ lifetime on addition of $Os(CN)_6^{4-}$ supports this hypothesis, which was previously advanced on the basis of the spectroscopic properties of the $[Eu\subset 2.2.1]^{3+}$–$M(CN)_6^{4-}$ ion pairs (M = Fe, Ru, Os).[27,28]

For the $[Ln\subset 2.2.1]^{3+}$–$2F^-$ species, neither intimate nor CN-bridged ion pairs are plausible in view of the smaller positive charge of the species and of the presence of F^- ions in the cryptand holes.[17] This picture is confirmed by the behavior of the IPCT band in the $[Eu\subset 2.2.1]^{3+}/Fe(CN)_6^{4-}$ system on addition of F^- anions. The presence of this band for F^- concentrations, corresponding to the formation of the $[Eu\subset 2.2.1]^{3+}$–F^- species,[17,26] indicates that a charge-transfer process from the iron hexacyanide to the europium species still takes place, presumably in a CN-bridged ion pair as for the $[Eu\subset 2.2.1]^{3+}/M(CN)_6^{4-}$ (M = Fe, Ru, Os) systems.[27,28] The decrease in intensity and the blue shift may be due to the smaller positive charge on the Eu species. This disappearance of the IPCT band when only the $[Eu\subset 2.2.1]^{3+}$–$2F^-$ species is present[17,26] indicates that in this case no CN-bridged ion pair is formed. Thus, only formation of outer-sphere ion pairs (Figure 3) is conceivable in the $[Ln\subset 2.2.1]^{3+}$–$2F^-/M(CN)_6^{z-}$ systems.

The trends shown by the quenching constants (Table II) can be at least in part rationalized on the basis of the three different types of precursor complexes discussed above (Figure 3):

(i) The quenching constants can never be diffusion controlled (point 6 above) because energy- or electron-transfer processes in the outer-sphere precursor complex are intrinsically nonadiabatic owing to the poor overlap of the f lanthanide orbitals with the orbitals of the reaction partner.[56] Inner-sphere processes possible for the Ln_{aq}^{3+} and $[Ln\subset 2.2.1]^{3+}$ species (Figure 3) may be intrinsically adiabatic, but they cannot be faster than the rate of formation of the bridged or intimate ion pairs.[57]

(ii) The strong decrease of the rate constants for energy-transfer quenching in the series $Ln_{aq}^{3+} > [Ln\subset 2.2.1]^{3+} > [Ln\subset 2.2.1]^{3+}$–$2F^-$ (point 1 above) can be accounted for on the basis of the involvement of intimate, CN-bridged, and outer-sphere precursor complexes, respectively, with the electronic factor decreasing along the series and controlling the rate of the process.

(iii) The increase in the energy-transfer rate in going from the $Tb_{aq}^{3+}/Cr(CN)_6^{3-}$ to the $Tb_{aq}^{3+}/Fe(CN)_6^{4-}$ system (point 3) can be accounted for by the fact that the rate of formation of the intimate ion pair is likely to increase with the increasing negative charge of the quencher. The opposite trend shown by the data concerning the $[Tb\subset 2.2.1]^{3+}$ and $[Tb\subset 2.2.1]^{3+}$–$2F^-$ systems with the same quenchers is indicative of formation of looser precursor complexes where the less solvated quencher ($Cr(CN)_6^{3-}$) may better approach the lanthanide species.

(iv) The rate of electron-transfer quenching of Eu_{aq}^{3+} and $[Eu\subset 2.2.1]^{3+}$ in the intimate and bridged ion pairs could be almost adiabatic and controlled by water displacement, whereas electron-transfer quenching of $[Eu\subset 2.2.1]^{3+}$–$2F^-$ is controlled by electronic factors in an outer-sphere complex (point 4).

(v) The observation reported under point 5 seems to suggest that the rate constant of energy-transfer processes is more sensitive to orbital overlap (and thus to center-to-center distance between the two species) than is that of electron transfer.

(vi) The insensitivity of the energy-transfer rate constants to the nature of the central lanthanide ion (point 2) suggests that metal–metal orbital coupling via nephelauxetic effects[58] or charge-transfer perturbations[12] has comparable (presumably very small) influence for the two lanthanide ions.

Acknowledgment. We thank Prof. G. Blasse for useful discussions concerning energy transfer. G. Gubellini and V. Cacciari are gratefully acknowledged for technical assistance. This work was supported by the Ministero della Pubblica Istruzione and Consiglio Nazionale delle Ricerche.

Registry No. Eu^{3+}, 22541-18-0; Tb^{3+}, 22541-20-4; $[Tb\subset 2.2.1]^{3+}$, 71238-22-7; $[Eu\subset 2.2.1]^{3+}$, 65013-29-8; $[Tb\subset 2.2.1]^{3+}$–$2F^-$, 110353-51-0; $[Eu\subset 2.2.1]^{3+}$–$2F^-$, 110316-49-9; $Cr(CN)_6^{3-}$, 14875-14-0; $Fe(CN)_6^{4-}$, 13408-63-4; $Co(CN)_6^{3-}$, 14897-04-2; $Ru(CN)_6^{4-}$, 21029-33-4; $Os(CN)_6^{4-}$, 19356-45-7.

(56) Balzani, V.; Scandola, F.; Orlandi, G.; Sabbatini, N.; Indelli, M. T. *J. Am. Chem. Soc.* **1981**, *103*, 3370.

(57) The rate constants of water exchange for tripositive lanthanide cations are on the order of 10^9 s^{-1}.[34,35]

(58) Gandolfi, M. T.; Maestri, M.; Sandrini, D.; Balzani, V. *Inorg. Chem.* **1983**, *22*, 3435.

Contribution from the Department of Chemistry and Laboratory for Molecular Structure and Bonding, Texas A&M University, College Station, Texas 77843

Tetramethyldiplatinum(III) (Pt–Pt) Complexes with 2-Hydroxypyridinato Bridging Ligands. 2. Reversals of Ligand Orientations[1]

Daniel P. Bancroft and F. Albert Cotton*

Received January 5, 1988

The compounds $[Pt_2(CH_3)_4(hp)_2(py)_2]$ and $[Pt_2(CH_3)_4(fhp)_2(py)_2]$, where hp represents the 2-hydroxypyridinate anion ($C_5H_4NO^-$) and fhp represents the 2-hydroxy-6-fluoropyridinate anion ($C_6H_3FNO^-$), can be converted to the corresponding monopyridine adducts by chromatography on silica gel. The surprising aspect of these conversions is that the arrangement of the hp and fhp ligands changes to head-to-head (HH) from head-to-tail (HT) and that, upon treatment with excess pyridine, the HH monopyridinates are reconverted to the HT bis(pyridine) adducts. The structures of $[Pt_2(CH_3)_4(hp)_2(py)]$ (**1**) and $[Pt_2(CH_3)_4(fhp)_2(py)]$ (**2**) were established by X-ray crystallography. Also reported here is the preparation of $[Pt_2(CH_3)_4(bhp)_2(py)]$ (**3**), where bhp = the 2-hydroxy-6-bromopyridinate anion. This has the expected HH structure. Crystallographic data are as follows. For **1**: $P\bar{1}$, $a = 9.637$ (2) Å, $b = 12.246$ (3) Å, $c = 8.573$ (3) Å, $\alpha = 85.71$ (3)°, $\beta = 91.98$ (3)°, $\gamma = 92.35$ (2)°, $Z = 2$ ($R = 0.030$; $R_w = 0.043$). For **2**: $P2_1/n$, $a = 9.458$ (3) Å, $b = 15.851$ (6) Å, $c = 14.156$ (4) Å, $\beta = 102.82$ (2)°, $Z = 4$ ($R = 0.030$; $R_w = 0.044$). For **3**: $P\bar{1}$, $a = 9.493$ (2) Å, $b = 13.198$ (4) Å, $c = 9.046$ (2) Å, $\alpha = 91.55$ (4)°, $\beta = 97.73$ (3)°, $\gamma = 92.33$ (4)°, $Z = 2$ ($R = 0.045$; $R_w = 0.057$).

Introduction

During the past two decades there has been a dramatic increase in the number of papers concerning the chemistry of platinum complexes where the platinum atoms are formally in the +3 oxidation state.[2,3] The majority of these complexes are binuclear and have either two or four bidentate ligands bridging the two d^7 metal centers. The coordination spheres are generally completed by the binding of two anionic or neutral donor ligands to the

(1) Part 1: Bancroft, D. P.; Cotton, F. A.; Falvello, L. R.; Schwotzer, W. *Inorg. Chem.* **1986**, *25*, 763.

(2) Woolins, D. J.; Kelly, P. F. *Coord. Chem. Rev.* **1985**, *65*, 115.

(3) O'Halloran, T. V.; Lippard, S. J. *Isr. J. Chem.* **1985**, *25*, 130.

0020-1669/88/1327-1633$01.50/0

Table I. Crystallographic Data and Parameters for $[Pt_2(CH_3)_4(xhp)_2(py)]$ (xhp = hp, fhp, and bhp)

	$[Pt_2(CH_3)_4(hp)_2(py)]$	$[Pt_2(CH_3)_4(fhp)_2(py)]$	$[Pt_2(CH_3)_4(bhp)_2(py)]$
formula			
fw	717.60	753.59	875.41
space group	$P\bar{1}$	$P2_1/n$	$P\bar{1}$
syst abs	none	$h0l$: $h + l = 2n + 1$ $0k0$: $k = 2n + 1$	none
a, Å	9.637 (2)	9.458 (3)	9.493 (2)
b, Å	12.246 (3)	15.851 (6)	13.198 (4)
c, Å	8.573 (3)	14.156 (4)	9.046 (2)
α, deg	85.71 (3)	90.0	91.55 (4)
β, deg	91.98 (3)	102.82 (2)	97.73 (3)
γ, deg	92.35 (2)	90.0	92.33 (4)
V, Å	1007.5 (5)	2069 (1)	1121.5 (8)
Z	2	4	2
D_{calcd}, g/cm^3	2.365	2.419	2.592
cryst size, mm	0.3 × 0.2 × 0.15	0.2 × 0.3 × 0.25	0.2 × 0.15 × 0.2
μ(Mo Kα), cm^{-1}	146.075	136.836	161.412
data collcn instrum	$P\bar{1}$	$P\bar{1}$	$P\bar{1}$
radiation (monochromated in incident beam)	Mo Kα (λ = 0.71073 Å)	Mo Kα (λ = 0.71073 Å)	Mo Kα (λ = 0.71073 Å)
orientation reflcns: no.; range (2θ), deg	15; 20.06–26.33	15; 18.10–28.69	15; 20.79–29.47
temp., °C	5	5	5
scan method	θ–2θ	θ–2θ	θ–2θ
data collcn range (2θ), deg	4.0–50.0	4.0–45.0	4.0–45.0
no. of unique data	3806	3027	2261
tot. no. with $F_o^2 > 3\sigma(F_o^2)$	2625	2099	1939
no. of params refined	235	253	253
transmissn factors: max; min	99.70%; 54.81%	98.92%; 58.64%	99.17%; 41.80%
R^a	0.030	0.030	0.045
$R_w{}^b$	0.043	0.044	0.057
quality-of-fit indicator^c	0.973	0.993	1.203
largest shift/esd, final cycle	0.98	0.37	0.05
largest peak, e/Å^3	0.855	0.902	1.556

$^a R = \sum||F_o| - |F_c||/\sum|F_o|$. $^b R = [\sum w(|F_o| - |F_c|)^2/\sum w|F_o|^2]^{1/2}$; $w = 1\sigma^2(|F_o|)$. ^{c}Quality of fit $= [\sum w(|F_o| - |F_c|)^2/(N_{observns} - N_{params})]^{1/2}$.

positions at either end of the Pt–Pt vector. Coordinatively unsaturated complexes, with one penta- and one hexa coordinate platinum atom, can be formed by removing one of the axial lgands. In the previous paper[1] we demonstrated that complexes of this type could be prepared by using bridging ligands with bulky substitutents that effectively block one axial position.[3] These complexes were prepared by the following reaction sequence:

$$[Pt_2(CH_3)_4(R_2S)_2] + 2Ag(xhp) \rightarrow [Pt_2(CH_3)_4(xhp)_2(R_2S)_n] + 2Ag$$

$$[Pt_2(CH_3)_4(xhp)_2(R_2S)_n] + \text{excess pyridine} \rightarrow [Pt_2(CH_3)_4(xhp)_2(py)_n] + 2R_2S$$

where R = C_2H_5, py = pyridine, and xhp$^-$ is a generic abbreviation for the class of bidentate, anionic ligands shown in diagram I. In

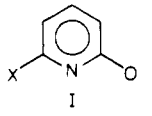

I

X	ligand symbol
H	hp
F	fhp
Cl	chp
CH_3	mhp
Br	bhp

another short notation to be employed here, HH and HT will be used to denote the head-to-head and head-to-tail ligand relationships illustrated in diagram II. The italic prefixes, *HH-* and *HT-*, can be used in writing names and formulas.

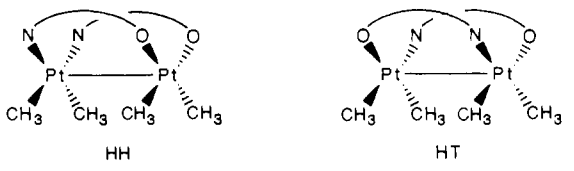

II

In our previous study of four $[Pt_2(CH_3)_4(xhp)_2(py)_n]$ species, we found that when the xhp ligands had small X groups (H, F), the xhp ligands adopted a HT arrangement and two pyridine molecules were coordinated, one at each axial position. On the other hand, for the larger X groups (Cl, CH_3), the xhp ligands adopted a HH arrangement and only one pyridine molecule was coordinated, namely, at the end opposite to that where the X groups were located. These observations seemed understandable on the basis of a steric argument, namely, that the larger X groups were so large that if one were to be placed at each end (in an HT structure) axial coordination would be weakened or prevented at both ends of the Pt_2^{6+} unit, whereas the HH arrangement at least allowed one good axial bond to be formed. The smaller X groups (H, F), however, are small enough to permit axial coordination at both ends when an HT disposition is adopted. In short, the observations appeared to have a simple explanation and the story seemed complete. We have now found that there are further ramifications to these systems.

We have found that the following processes can occur:

$$\underset{\text{pale yellow}}{[Pt_2(CH_3)_4(xhp)_2(py)_2]} \underset{+py}{\overset{-py}{\rightleftharpoons}} \underset{\text{orange-red}}{[Pt_2(CH_3)_4(xhp)_2(py)]}$$

xhp = hp or fhp

In the forward reaction the pyridine molecule is removed simply by subjecting the compound to chromatography on a silica gel column and evaporating the eluant to dryness. The reaction is reversed by the addition of excess pyridine to a solution of the monopyridine complex. The important and surprising feature of these processes is that they involve reversible HH $\rightleftharpoons$ HT conversions along with the loss and gain of axial pyridine molecules. The equilibria and mechanism of the ligand reversals are still unknown but are under investigation.[4] In the meantime, we report here the complete synthetic details as well as X-ray structural characterization of the new monopyridine HH complexes. In addition, we have synthesized and structurally characterized another complex, which does not undergo the reversible rearrangement of the bridging ligands, namely *HH*-$Pt_2(CH_3)_4$-$(bhp)_2$py. We report on this first bhp (2-hydroxy-6-bromo-

(4) Abbott, E. H., Montana State University, private communication.

Table II. Positional Parameters and Their Estimated Standard Deviations for $[Pt_2(CH_3)_4(hp)_2(py)]$

atom	*x*	*y*	*z*	*B*,[a] Å^2
Pt(1)	0.82186 (4)	0.15317 (3)	0.27419 (4)	2.203 (7)
Pt(2)	0.87730 (4)	0.32013 (3)	0.08643 (4)	2.548 (8)
O(1)	0.6865 (7)	0.2616 (5)	0.3762 (8)	2.8 (1)
O(2)	0.6562 (8)	0.1152 (6)	0.1103 (8)	3.3 (2)
N(1)	0.8190 (9)	0.4070 (6)	0.278 (1)	2.6 (2)
N(2)	0.6657 (8)	0.2965 (7)	0.0172 (9)	2.7 (2)
N(3)	0.7416 (8)	0.0335 (6)	0.426 (1)	2.5 (2)
C(1)	0.726 (1)	0.3622 (8)	0.381 (1)	2.5 (2)
C(2)	0.327 (1)	0.5750 (9)	0.503 (1)	3.8 (3)
C(3)	0.723 (1)	0.533 (1)	0.507 (1)	4.3 (3)
C(4)	0.823 (1)	0.5799 (9)	0.400 (1)	3.7 (2)
C(5)	0.865 (1)	0.5130 (9)	0.295 (1)	3.2 (2)
C(6)	0.598 (1)	0.1974 (8)	0.033 (1)	2.6 (2)
C(7)	0.461 (1)	0.183 (1)	0.966 (1)	3.4 (2)
C(8)	0.603 (1)	0.727 (1)	0.110 (1)	3.5 (2)
C(9)	0.531 (1)	0.625 (1)	0.123 (1)	3.4 (2)
C(10)	0.401 (1)	0.6178 (9)	0.063 (1)	3.3 (2)
C(11)	0.697 (1)	0.9350 (9)	0.372 (1)	3.2 (2)
C(12)	0.629 (1)	0.8572 (9)	0.472 (2)	4.0 (3)
C(13)	0.394 (1)	0.122 (1)	0.373 (2)	4.2 (3)
C(14)	0.344 (1)	0.023 (1)	0.320 (1)	3.9 (3)
C(15)	0.277 (1)	0.9459 (9)	0.421 (1)	3.2 (2)
C(16)	0.948 (1)	0.047 (1)	0.180 (1)	3.9 (2)
C(17)	0.979 (1)	0.183 (1)	0.431 (1)	3.6 (2)
C(18)	0.077 (1)	0.755 (1)	0.111 (1)	4.1 (3)
C(19)	0.086 (1)	0.352 (1)	0.133 (1)	4.2 (3)

[a] *B* values for anisotropically refined atoms are given in the form of the isotropic equivalent thermal parameter defined as $(4/3)[a^2B(1,1) + b^2B(2,2) + c^2B(3,3) + ab(\cos\gamma)B(1,2) + ac(\cos\beta)B(1,3) + bc(\cos\alpha)B(2,3)]$.

pyridinate anion) complex here.

Experimental Section

The silver salts of Hhp and Hfhp were prepared by the previously published method.[1] Ag(bhp) was prepared in a similar manner. Hbhp was obtained by hydrolysis of 2,6-dibromopyridine in a *t*-BuOK/*t*-BuOH mixture according to a literature method.[5] We thank Dr. M. Matusz for giving us a sample.

Preparation of *HH*-$[Pt_2(CH_3)_4(hp)_2(py)]$ (1). *HT*-$[Pt_2(CH_3)_4(hp)_2(py)_2]$[1] (2.0 g, 2.5 mmol) was dissolved in 30 mL of chloroform and chromatographed on a silica gel column (Mallinckrodt, Silicar, Grade 62, 60–200 mesh) prepared with a 1:1 (v/v) mixture of chloroform/toluene. Elution of the sample with a 3:1 (v/v) mixture of chloroform/toluene yielded an orange solution, which deposited crystals of composition $[Pt_2(CH_3)_4(hp)_2(py)]$ when concentrated and cooled at −10 °C for several days. If the sample was eluted with a 1:1 mixture of pyridine/toluene, $[Pt_2(CH_3)_4(hp)_2(py)_2]$ could be obtained in essentially quantitative yields.

Preparation of *HH*-$[Pt_2(CH_3)_4(fhp)_2(py)]$ (2). A sample of *HT*-$[Pt_2(CH_3)_4(fhp)_2(py)_2]$, prepared by the previously described method,[1] was chromatographed on a silica gel column as described above. Refrigeration at −10 °C of a concentrated sample of the eluant for several days yielded large single crystals of *HH*-$[Pt_2(CH_3)_4(fhp)_2(py)]$ and a small amount of unreacted *HT*-$[Pt_2(CH_3)_4(fhp)_2(py)_2]$. *HH*-$[Pt_2(CH_3)_4(fhp)_2(py)]$ could be obtained in pure form by again subjecting it to chromatography followed by evaporation of the eluant to dryness in vacuum. Microscopic examination of a crystalline sample prepared in this manner revealed only orange-red crystals of *HH*-$[Pt_2(CH_3)_4(fhp)_2(py)]$.

Preparation of *HH*-$[Pt_2(CH_3)_4(bhp)_2(py)]$ (3). A suspension of $[Pt_2(CH_3)_4((C_2H_5)_2S)_2]$[6] (0.12 g, 0.19 mmol) and Ag(bhp) (0.11 g, 0.38 mmol) in 20 mL of dry benzene was stirred at room temperature for 72 h. The colloidal Ag was removed by vacuum filtration through Celite and the remaining red-orange solution was evaporated to dryness in vacuum. Excess pyridine (ca. 10 mL) was added, and the solution was subsequently filtered after being stirred at room temperature for several hours. The excess pyridine was then removed in vacuum, leaving an orange-red oil. The oil was dissolved in a minimal amount of chloroform (ca. 10 mL) and subsequently purified by flash chromatography on a silica gel column prepared as described above. Orange crystals of *HH*-$[Pt_2(CH_3)_4(bhp)_2(py)]$ were grown by slow evaporation of the eluant in air.

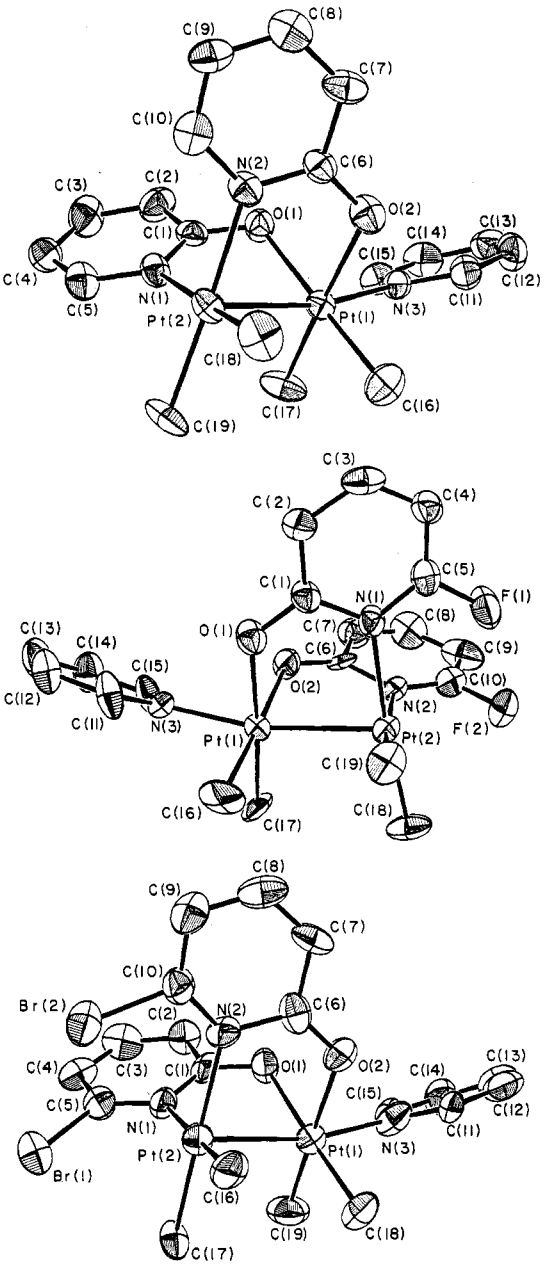

Figure 1. Molecular structures of $[Pt_2(CH_3)_4(hp)_2(py)]$ (top), $[Pt_2(CH_3)_4(fhp)_2(py)]$ (middle), and $[Pt_2(CH_3)_4(bhp)_2(py)]$ (bottom). Atoms are represented by their thermal displacement ellipsoids contoured at the 50% probability level.

X-ray Crystallography. None of the three structures presented any unusual problem. All were solved and refined routinely by following standard procedures. The crystallographic parameters and procedural data are summarized for all three structures in Table I. For **1** and **2**, metal atom coordinates were obtained from the Patterson function and for **3** the direct-methods program Multan 11/82 was used. In each case the other atoms were then located in an alternating series of difference electron density maps and least-squares refinements. All three structures were refined to satisfactorily low residuals by treating all atoms anisotropically while omitting hydrogen atoms entirely. Absorption corrections were made in each case by the use of ψ-scan data, and for **2** and **3** also by using the Difabs program.[7]

Only the principal dimensions of the molecules are reported here, but complete listings are provided in the supplementary material (see paragraph at the end of the paper).

Description of the Structures. *HH*-$[Pt_2(CH_3)_4(hp)_2(py)]$ (1). An

(5) Newkomb, G. R.; Brousard, J.; Seatres, S. K.; Sauer, J. D. *Synthesis* **1974**, 706.

(6) Kuyper, J; vander Laan, R.; Jeanneaus, F.; Vrieze, K. *Transition Met. Chem. (Weinheim, Ger.)* **1976**, *1*, 199.

(7) Walker, N.; Stuart, D. *Acta Crystallogr., Sect. A: Found. Crystallogr.* **1983**, *39*, 158.

Table III. Selected Bond Distances and Bond Angles for $[Pt_2(CH_3)_4(xhp)_2(py)]$ (xhp = hp, fhp, chp, bhp, mhp)[a]

Distances (Å)

compd	x	Pt–Pt	Pt–C	Pt–N	Pt–O	Pt–N_{ax}	ref
1	H	2.556 (1)	2.05 [1]	2.122 [4]	2.150 [1]	2.034 (8)	this work
2	F	2.554 (1)	2.03 [1]	2.15 [1]	2.156 [9]	2.043 [10]	this work
3	Br	2.551 (1)	2.03 [1]	2.18 [4]	2.152 [7]	2.06 (2)	this work
4	Cl	2.543 (1)	2.04 [1]	2.168 [5]	2.14 [1]	2.060 (11)	1
5	CH_3	2.545 (1)	2.05 [1]	2.158 [4]	2.132 [4]	2.030 (8)	1

Angles (deg)

	compd				
	1	**2**	**3**	**4**	**5**
Pt–Pt–N_{ax}	168.9 (2)	167.8 (3)	168.5 (5)	169.0 (4)	167.2 (2)
Pt–Pt–O	85.0 [1]	85 [1]	84 [1]	85 [1]	83.2 [4]
Pt–Pt–N	82.6 [2]	85.3 [8]	84 [1]	84.2 [6]	84.6 [1]
Pt–Pt–C[b]	102 [1]	100 [1]	97.8 [8]	99.2 [2]	98.4 [4]
Pt–Pt–C[c]	96.6 [9]	98.0 [8]	97.2 [6]	96.8 [1]	97.7 [1]
C–Pt–Pt–C	27 [3]	21 [2]	28 [1]	27.2 [1]	31 [2]
O–Pt–Pt–N	25 [2]	17 [2]	24 [2]	22 [1]	25 [1]

[a] Estimated standard deviations shown in least significant digits are shown in parentheses. [b] Trans to N. [c] Trans to O.

ORTEP view of the molecule is shown in Figure 1. Table II contains the final positional and thermal parameters and Table III lists selected bond lengths and angles. The molecular structure consists of a binuclear Pt(III) molecule with a Pt–Pt single bond distance of 2.556 (1) Å. The two hp^- ligands bridge the platinum atoms in a head-to-head manner, and one of the axial positions is unoccupied. The axial pyridine molecule is coordinated to the platinum atom having bonds to the oxygen atoms of the hp^- ligands, bonds to two cis-oriented methyl groups, and a bond to the other platinum atom. The Pt–N_{ax} distance is short, 2.034 (8) Å, indicating that the pyridine molecule is strongly coordinated. The cis methyl groups on the respective platinum centers interact sterically, causing a substantial torsional twist about the Pt–Pt vector. The pyridine molecule also interacts sterically with its adjacent methyl groups, which force the pyridine molecule to bend away from the Pt–Pt vector by about 11°. Finally, although the torsional twist about the Pt–Pt vector alleviates some of the steric strain between the methyl groups, there still appears to be steric strain in the molecule as evidenced by the Pt–Pt–C angles of 101.8 [16] and 96.6 [9]° for the penta- and hexacoordinate platinum atoms, respectively. Although the methyl groups experience considerable steric interactions, there appears to be no weakening of the Pt–C bonds, which have an average length of 2.04 [8] Å.

***HH*-$[Pt_2(CH_3)_4(fhp)_2(py)]$ (2).** An ORTEP view of the molecule is shown in Figure 1. Table IV contains the final positional and thermal parameters, and Table III lists selected bond lengths and angles. The structure is very similar to that of $[Pt_2(CH_3)_4(hp)_2(py)]$ described above. The Pt–Pt bond distance, 2.554 (1) Å, is identical within experimental error with the distance in the analogous hp^--bridged complex. The Pt_2 unit is bridged by two fhp^- ligands that are oriented in the head-to-head manner. The axial position opposite to the end of the molecule with the fluorine atoms is occupied by a molecule of pyridine, while the other axial position is unoccupied. As before, the pyridine molecule is strongly coordinated with a Pt–N_{ax} distance of 2.043 (10) Å. The Pt–Pt–N_{ax} bond angle is 167.3° with the pyridine molecule bent away from the adjacent methyl groups. The partially staggered conformation, which is present in all of these complexes due to the steric interactions between the methyl groups, is also observed here and is characterized by a C–Pt–Pt–C torsional angle of 21 [2]°. The Pt–Pt–C bond angles for the penta- and hexacoordinate platinum atoms are similar to those of the analogous hp^--bridged complex and are 100 [1] and 98.0 [8]°, respectively. The average Pt–O_{hp} bond lengths are 2.146 [11] and 2.156 [9] Å, respectively, while the average Pt–C bond length is 2.03 [1] Å.

***HH*-$[Pt_2(CH_3)_4(bhp)_2(py)]$ (3).** An ORTEP view of the molecule is shown in Figure 1. Table V contains the final positional and thermal parameters, and selected bond lengths and angles are included in Table III. The molecular structure is similar to those of the hp^-- and fhp^--bridged complexes described above and to those of the mhp and chp compounds previously reported.[1] The binuclear Pt(III) molecule has a Pt–Pt bond distance of 2.550 (1) Å. The platinum atoms are bridged by two bhp^- ligands, which are arranged in a polar manner with the bromine atoms effectively blocking one axial site. The other axial coordination site is occupied by a molecule of pyridine with a Pt–N_{ax} distance of 2.031 (10) Å. As before, the pyridine molecule is bent away from the methyl groups by about 12°. The average C–Pt–Pt–C torsion angle due to steric repulsion between the methyl groups in the two equatorial coordination planes is 28[1]°. The average Pt–C bond length is 2.03 [1] Å.

Table IV. Positional Parameters and Their Estimated Standard Deviations for $[Pt_2(CH_3)_4(fhp)_2(py)]$

atom	*x*	*y*	*z*	*B*,[a] Å^2
Pt(1)	0.67108 (5)	0.08459 (3)	0.24611 (3)	2.16 (1)
Pt(2)	0.86385 (5)	0.03304 (3)	0.15868 (3)	2.35 (1)
F(1)	1.1590 (8)	−0.0364 (5)	0.2409 (6)	4.7 (2)
F(2)	1.1328 (8)	0.1171 (6)	0.1166 (5)	4.4 (2)
O(1)	0.7466 (9)	−0.0145 (5)	0.3491 (6)	3.0 (2)
O(2)	0.8385 (8)	0.1662 (6)	0.3215 (6)	3.0 (2)
N(1)	0.958 (1)	−0.0265 (6)	0.2945 (7)	2.5 (2)
N(2)	0.983 (1)	0.1452 (7)	0.2152 (6)	2.4 (2)
N(3)	0.552 (1)	0.1239 (7)	0.3417 (6)	2.6 (2)
C(1)	0.875 (1)	−0.0448 (8)	0.3607 (9)	2.6 (3)
C(2)	0.939 (1)	−0.0909 (9)	0.4433 (9)	3.4 (3)
C(3)	1.083 (2)	−0.1194 (9)	0.4542 (9)	3.6 (3)
C(4)	1.161 (1)	−0.1010 (9)	0.3883 (9)	3.2 (3)
C(5)	1.090 (1)	−0.057 (1)	0.3110 (9)	3.4 (3)
C(6)	0.949 (1)	0.1896 (8)	0.2918 (7)	2.2 (3)
C(7)	1.042 (1)	0.2565 (9)	0.3319 (9)	3.4 (3)
C(8)	1.157 (2)	0.2776 (9)	0.300 (1)	4.3 (4)
C(9)	1.197 (2)	0.230 (1)	0.225 (1)	4.8 (4)
C(10)	1.103 (1)	0.1667 (9)	0.1897 (9)	3.6 (3)
C(11)	0.465 (1)	0.0671 (9)	0.377 (1)	3.9 (3)
C(12)	0.397 (1)	0.0903 (9)	0.451 (1)	4.1 (3)
C(13)	0.415 (1)	0.170 (1)	0.490 (1)	4.2 (3)
C(14)	0.498 (1)	0.2282 (9)	0.451 (1)	3.9 (3)
C(15)	0.566 (1)	0.2033 (8)	0.377 (1)	3.3 (3)
C(16)	0.502 (2)	0.014 (1)	0.174 (1)	4.9 (4)
C(17)	0.591 (1)	0.1809 (9)	0.1532 (8)	3.4 (3)
C(18)	0.790 (2)	0.0823 (9)	0.0248 (9)	3.8 (3)
C(19)	0.775 (2)	−0.0776 (8)	0.110 (1)	3.8 (3)

[a] *B* values for anisotropically refined atoms are given in the form of the isotropic equivalent thermal parameter defined as $(4/3)[a^2B(1,1) + b^2B(2,2) + c^2B(3,3) + ab(\cos\gamma)B(1,2) + ac(\cos\beta)B(1,3) + bc(\cos\alpha)B(2,3)]$.

Discussion

The principal observation reported here is that $Pt_2(CH_3)_4(xhp)_2$ moieties with small X groups are not restricted to the HT stereochemistry with a ligand at each end, i.e., *HT*-$Pt_2(CH_3)_4(xhp)_2L_2$, as previously appeared to be the case. Rather, when there is a deficit of ligand L, they will adopt the *HH*-$Pt_2(CH_3)_4(xhp)_2L$ structure. We have shown here that these two types can be interconverted quite easily, and we have provided detailed structural characterization of the two new *HH*-$[Pt_2(CH_3)_4(xhp)_2(py)]$ compounds, namely, those with xhp = hp and fhp.

Three further questions are of interest.

(1) What are the equilibrium constants for the rearrangement processes in solution, i.e., for reactions of type (1)?

HT-$[Pt_2(CH_3)_4(xhp)_2(py)_2]$ = *HH*-$[Pt_2(CH_3)_4(xhp)_2(py)]$ + py (1)

Table V. Positional Parameters and Their Estimated Standard Deviations for $[Pt_2(CH_3)_4(bhp)_2(py)]$

atom	x	y	z	B,[a] Å²
Pt(1)	0.81413 (8)	0.14160 (6)	0.79609 (9)	3.07 (2)
Pt(2)	0.85735 (8)	0.28676 (6)	0.62480 (9)	3.01 (2)
Br(1)	0.9654 (3)	0.5434 (2)	0.7033 (3)	4.84 (5)
Br(2)	0.6750 (3)	0.4491 (2)	0.4248 (3)	4.67 (6)
O(1)	0.686 (1)	0.249 (1)	0.893 (1)	3.5 (3)
O(2)	0.628 (1)	0.103 (1)	0.637 (2)	3.9 (3)
N(1)	0.809 (2)	0.383 (1)	0.814 (2)	3.2 (4)
N(2)	0.634 (2)	0.268 (1)	0.547 (2)	3.1 (4)
N(3)	0.738 (2)	0.034 (1)	0.929 (2)	4.0 (4)
C(1)	0.718 (2)	0.343 (2)	0.904 (2)	3.1 (4)
C(2)	0.662 (2)	0.406 (2)	1.007 (2)	3.4 (5)
C(3)	0.703 (2)	0.508 (2)	1.021 (2)	4.7 (6)
C(4)	0.792 (2)	0.551 (2)	0.930 (2)	3.9 (5)
C(5)	0.839 (2)	0.486 (2)	0.830 (2)	3.7 (5)
C(6)	0.566 (2)	0.172 (2)	0.569 (2)	3.6 (5)
C(7)	0.415 (2)	0.158 (2)	0.499 (2)	4.0 (5)
C(8)	0.349 (2)	0.232 (2)	0.421 (2)	4.5 (6)
C(9)	0.421 (2)	0.324 (2)	0.396 (2)	4.2 (5)
C(10)	0.563 (2)	0.331 (2)	0.459 (2)	3.6 (5)
C(11)	0.686 (2)	−0.057 (2)	0.872 (3)	4.7 (6)
C(12)	0.619 (2)	−0.125 (2)	0.958 (3)	5.2 (6)
C(13)	0.611 (2)	−0.106 (2)	1.106 (2)	4.6 (6)
C(14)	0.672 (2)	−0.013 (2)	1.172 (3)	4.8 (6)
C(15)	0.734 (2)	0.056 (2)	1.077 (2)	3.2 (5)
C(16)	0.892 (2)	0.203 (2)	0.443 (3)	4.5 (6)
C(17)	1.072 (2)	0.300 (2)	0.678 (2)	3.5 (4)
C(18)	0.931 (2)	0.036 (2)	0.703 (2)	4.2 (5)
C(19)	0.983 (2)	0.175 (2)	0.951 (3)	5.3 (6)

[a] *B* values for anisotropically refined atoms are given in the form of the isotropic equivalent thermal parameter defined as $(4/3)[a^2B(1,1) + b^2B(2,2) + c^2B(3,3) + ab(\cos\gamma)B(1,2) + ac(\cos\beta)B(1,3) + bc(\cos\alpha)B(2,3)]$.

(2) By what mechanism or pathway do the HT and HH arrangements interconvert?

(3) How can we rationalize the fact that the HT structure with two axial ligands and the HH structure with only one are thermodynamically competitive in certain cases but not in others?

We are seeking answers to the first two questions by NMR studies of solutions, but these are still incomplete. We can, however, offer a reasonably thorough discussion of the third question, as follows. With respect to compounds containing xhp^- ligands with bulky X groups, the view that they will show a marked preference for the HH arrangement remains valid and is reinforced by the results reported here on the new bhp^- derivative. This is because, as noted before,[1] an HT arrangement would presumably prevent axial ligation altogether, and thus we have a "half a loaf is better than none" situation; namely, the one good axial ligand bond attainable with the HH arrangement is better than no axial bonds at all. However, there is now an interesting question that we have not explicitly considered before: Is it possible that under conditions where the $Pt_2(CH_3)_4(xhp)_2$ unit is denied access to *any* potential axial ligand, the *HT*-$[Pt_2(CH_3)_4(xhp)_2]$ molecules might be formed regardless of the size of the substituent X? Could we, for example, treat one of the *HH*-$[Pt_2(CH_3)_4(xhp)_2(py)]$ complexes with a Lewis acid capable of competitively removing the py ligand and thus obtain a product devoid of axial ligands? If so, would there be an accompanying rearrangement to the HT type of structure? We plan to undertake experiments that address this question.

The results reported here have significantly enlarged our understanding of the behavior of $Pt_2(CH_3)_4(xhp)_2L_n$ systems, where xhp is one of the ligands that is relatively undemanding sterically, viz., hp^- or fhp^-. In terms of (1) we had previously made the tacit assumption that the equilibrium would lie so far to the left as to make only the one type of product available. This appeared reasonable on the assumption that there is probably not much difference in the inherent stabilities of the *HH*-$[Pt_2(CH_3)_4(xhp)_2]$ and *HT*-$[Pt_2(CH_3)_4(xhp)_2]$ arrangements. Thus, the simple fact that for small X the latter could bind two axial ligands while the former could bind only one would obviously favor the HT type of structure. The new results show that the situation is not so extreme, and we must now ask why. It may be that the HH arrangement of xhp^- ligands is actually more favorable than the HT arrangement, but we do not see why this should be so, at least to any great degree. We are disposed to give decisive weight to the fact that the one axial ligand bond in the *HH*-$[Pt_2(CH_3)_4(xhp)_2(py)]$ isomers is, on the basis of bond length data, appreciably stronger than either of the axial bonds in the *HT*-$[Pt_2(CH_3)_4(xhp)_2(py)_2]$ molecules. The Pt–N_{py} bond lengths in all five *HH*-$[Pt_2(CH_3)_4(xhp)_2(py)]$ molecules are in the range 2.03–2.06 Å, whereas those in the two *HT*-$[Pt_2(CH_3)_4(xhp)_2(py)_2]$ cases are in the range 2.16–2.21 Å. While we are by no means suggesting that this difference implies that one bond in the former range is as strong as two in the latter range, there is clearly a contribution here toward making the HH situation competitive. When this is coupled with experimental conditions in which py lost from the dipyridine adduct is removed, it becomes plausible that the equilibrium in (1) can be shifted all the way to the right. However, the quantitative thermodynamic and the mechanistic aspects of the equilibria represented by (1) still need to be clarified.

Acknowledgment. We thank the National Science Foundation for support.

Registry No. **1**, 113778-08-8; **2**, 113778-10-2; **3**, 113778-09-9; *HT*-$[Pt_2(CH_3)_4(hp)_2(py)_2]$, 100351-35-7; *HT*-$[Pt_2(CH_3)_4(fhp)_2(py)_2]$, 100351-36-8; $[Pt_2(CH_3)_4((C_2H_5)_2S)_2]$, 62343-09-3; Ag(bhp), 113778-11-3.

Supplementary Material Available: Complete tables of bond distances, bond angles, general temperature factors, and torsional angles (15 pages); listings of observed and calculated structure factors (35 pages). Ordering information is given on any current masthead page.